

# Linear and nonlinear optical properties in single $\text{CuIn}_{1-x}\text{Ga}_x\text{Se}_2$ nanowire: Effects of size, incident intensity, relaxation time and Ga concentration

M. Rzaizi\*, M.S. El Kazdir, M. EL Khou, A. Oueriagli, and D. Abouelaoualim

*Cadi Ayyad University, Faculty of Sciences Semlalia, Physics Department,  
Marrakech, Morocco 40000 P.O.Box 2390.*

*\*e-mail: mouradrz1@gmail.com*

Received 17 September 2021; accepted 13 December 2021

The linear and nonlinear optical properties of  $\text{CuIn}_{1-x}\text{Ga}_x\text{Se}_2$  free standing nanowire have been studied by employing the compact-density matrix formalism and the effective mass approximation. Considering the system under the effect of the polarization vector of the incident light in both cases perpendicular and parallel to the axis of the nanowire, the systematic theoretical investigation contains results with all possible combinations of the involved parameters, such as incident light intensity, relaxation time, nanowire radius and Ga concentration. Our results show that in the case of the polarization vector perpendicular to the nanowire axis, the linear and nonlinear absorption coefficient and refractive index changes can be controlled by changing the nanowire radius, and the effect of Ga concentration is clearly apparent. In contrast, polarization along the nanowire axis allows for a very large absorption coefficient and control of the optical properties through the height, but minimal effect on the transition energy. The increase of the relaxation time as well as the intensity of the incident light has a major role in the nonlinearity effects, while the Ga concentration and the size of the structure influence the amplitude and the transition energy shift.

**Keywords:** Nanowires; nonlinear optical susceptibility; polarisation; optical absorption; refractive index; quantum confinement.

DOI: <https://doi.org/10.31349/RevMexFis.68.031001>

## 1. Introduction

Recent developments and advances in modern technology, both theoretical and experimental, have made it possible to scale electronics to the nanoscale, which could enable new functions and increased performance [1]. One-dimensional nanostructures in which charge carriers are confined in the other two dimensions are nanowires (NWs) [2, 3].

With physical and optical properties that are expected to be quite different and improved over bulk crystals due to the reduction in size, combined with the semiconducting properties of the materials, semiconductor nanowires have multiple qualities that are needed for future applications. Among the many advantages of nanowire geometry are high efficiency, high surface-to-volume ratio, high multi-material selectivity for efficient charge carrier extraction after light absorption [4], high light trapping in high-density nanowire arrays [5], quantum size effects (QSE), and size-dependent band gap that confer unique photoluminescence properties [6].

In recent years, considerable experimental [7, 8] and theoretical work has been devoted to semiconductor nanostructures in which charge carriers are confined in one, two, or three directions [9, 10]. Nanowires have a significant role both experimentally and theoretically. They are used as interconnects and functional units in nanoscale electronic, optoelectronic, electrochemical and electromechanical devices. Nanowires are integrated for applications such as high mobility transistors [11], light emitting diodes [12], biochemical sensors [13], and other applications. Due to their promising properties [14–17], nanowires are opening up new areas of research in the field of nanomaterials [18].

The strong polarization dependence of nanowires in light absorption and emission is one of the main challenges to their optimal technological integration. Indeed, nanowires have a highly anisotropic polarization response in both light absorption and emission. Light absorption is favored for light polarization along the axis of the nanowire, with little dependence on diameter [19, 22]. However, it is almost transparent for incident light exhibiting polarization perpendicular to its axis. This results in nearly half of the incoming white light passing through a nanowire without interaction with the material [20]. This anisotropy limits the use of nanowires in some photonic applications, such as photodetectors and solar cells [21]. Thus, the study of the effect of polarization on the optical properties of nanowires is a key element to compensate for the limitations encountered, and optimize their use in photonic applications requiring radial polarization of the incident light.

Among the multiple semiconductor compounds is the I-III-VI<sub>2</sub> family, including  $\text{CuIn}_{1-x}\text{Ga}_x\text{Se}_2$  (CIGS), which has been widely used in photovoltaics due to its many advantages. These include its direct band gap, high absorption coefficients for visible light with wavelengths up to about  $10^5 \text{ cm}^{-1}$  and its long-term optoelectronic stability [23–26]. In addition, the direct bandgap energy of CIGS can be tuned by varying the Gallium composition ratio,  $x = \text{Ga}/(\text{In} + \text{Ga})$  [27, 28]. The optical properties of these structures are very attractive to researchers both on an experimental and theoretical level. Although widely studied by many authors, optical transitions between subbands and between quantized energy levels remain one of the most crucial aspects of nanostructures. They are at the basis of several applications such as

infrared lasers and electro-optical modulators [29, 30]. As the quantum confinement increases, the energy difference between the sub-bands changes which has a direct impact on the linear and non-linear optical properties. These include changes in the linear and non-linear absorption coefficient as well as the refractive index changes, which can also be significantly modified and influenced by the parameters of the system under study. It is worth mentioning that second-order nonlinearities occur in noncentrosymmetric structures, while third-order optical nonlinearities occur in centro- and non-centrosymmetric nanostructures [31–37].

The aim of this paper is to investigate the effect of incident light intensity, relaxation time, nanowire radius and *Ga* mole fraction  $x$  on the linear, nonlinear and total parts of the two optical properties absorption coefficients (AC) and refractive index change (RI) in the free  $\text{CuIn}_{1-x}\text{Ga}_x\text{Se}_2$  nanowire and this for the two cases of polarization of the incident light: parallel and perpendicular to its axis. The electron is considered confined in an infinite cylindrical quantum well delimited by the structure boundaries. The intersubband electronic transition from the ground state to the first excited state is considered for each polarization. We expect that this work will be of great help in describing and understanding the correct behavior of optical properties in core-shell quantum dots (CSQDs) of different sizes and geometries in combination with the polarization dependence of the external excitation, which can be useful in technological applications such as nanowire-based radial and axial junction solar cells and photo-detectors. The paper is organized as follows: In Sec. 2, the proposed model is described and analytical expressions for the linear and nonlinear optical absorption coefficients and refractive index changes under the effective mass approximation and the density matrix approach are presented. Numerical results and discussions are given in Sec. 3. A brief conclusion is finally presented in Sec. 4, followed by references.

## 2. Theoretical Framework

In this work, we consider a free cylindrical  $\text{CuIn}_{1-x}\text{Ga}_x\text{Se}_2$  nanowire surrounded by vacuum. The potential distribution is taken as

$$V(r, \varphi) = \begin{cases} 0 & \text{for } r \leq R \\ \infty & \text{for } r > R \end{cases}.$$

There are two distinct regions that consist of a cylindrical potential well inside the wire where  $R$  is the radius, and outside the structure an infinite potential value is considered. The Schrodinger equation written in cylindrical coordinates  $(r, \varphi, z)$  with the Laplace operator for an electron confined inside the system under study is given as follows

$$\left( -\frac{\hbar^2}{2m^*} \left[ \frac{\partial^2}{\partial r^2} + \frac{1}{r} \frac{\partial}{\partial r} + \frac{1}{r^2} \frac{\partial^2}{\partial \varphi^2} + \frac{\partial^2}{\partial z^2} \right] + V(r, \varphi) \right) \times \psi(r, \varphi, z) = E \psi(r, \varphi, z). \quad (1)$$

Where  $m^*$  is the effective mass. Since the geometry of our system has axial symmetry, and given the selection rules, the allowed transitions are those between states with the same azimuthal quantum number. Therefore, considering the above potential distribution, the Schrodinger equation for our symmetry depends only on the height and the radius coordinates  $(r, z)$  such that

$$\left( -\frac{\hbar^2}{2m^*} \left[ \frac{\partial^2}{\partial r^2} + \frac{1}{r} \frac{\partial}{\partial r} + \frac{1}{r^2} \frac{\partial^2}{\partial \varphi^2} + \frac{\partial^2}{\partial z^2} \right] \right) \times \psi(r, z) = E \psi(r, z). \quad (2)$$

The energy levels  $E$  and the corresponding wave functions can be obtained by solving the Schrodinger equation. The radial wave function is the solution of the following equation

$$\left( r^2 \frac{\partial^2 \psi(r)}{\partial r^2} + r \frac{\partial \psi(r)}{\partial r} + \left[ \frac{2m^*}{\hbar^2} E_n r^2 \right] \right) \psi(r) = 0. \quad (3)$$

This leads to the radial wave function where  $\alpha_{lm}$  is the number  $l$  root of the Bessel function  $J$  and its order  $m$ , and  $k_{ml} = \alpha_{lm}/R$  the quantization condition of the wave vector  $k$ .

$$\psi(r) = J_m \left( \frac{\alpha_{lm}}{R} r \right). \quad (4)$$

Once the energies and their corresponding three-dimensional wave functions in cylindrical coordinates are obtained, we can calculate the energy difference between the ground state and the first excited state.

The process of photon absorption in low-dimensional systems, for a two-level electronic system, is defined as an optical transition between an initial state,  $i$ , and a final state,  $f$ , by absorption of a photon. Absorption of incident radiation is possible only if the energy of the radiation,  $\hbar\omega$ , coincides with the energy difference between the two states between which transitions are possible. The first- and third-order components of the absorption coefficient as well as the refractive index change of a crystal can be derived by the density matrix approach in conjunction with the perturbation expansion method [38–41].

We consider the system under the effect of an electromagnetic field  $\tilde{E}$  of frequency  $\omega$ , such that

$$E(t) = \tilde{E} e^{i\omega t} + \tilde{E}^* e^{-i\omega t}. \quad (5)$$

Which is incident with a polarization vector perpendicular to the axis of the nanowire. The electronic polarization of the system,  $p(t)$ , caused by the incident field,  $E(t)$ , can be written as follows [42]

$$p(t) = \epsilon_0 \chi(\omega) \tilde{E} e^{i\omega t} + \epsilon_0 \chi(-\omega) \tilde{E}^* e^{-i\omega t}. \quad (6)$$

Where  $\epsilon_0$  is the electrical permittivity of free space and  $\chi(\omega)$  is the Fourier component of the susceptibility of the

system. The electronic polarization will also be a series expansion, and by considering the system confined to two-level electronic transitions, the induced electric polarization up to third order in  $E$ , can be written as [43]

$$p(t) = \left( \epsilon_0 \chi_\omega^{(1)} \tilde{E} e^{i\omega t} + \epsilon_0 \chi_0^{(2)} \tilde{E}^2 + \epsilon_0 \chi_{2\omega}^{(2)} \tilde{E} e^{2i\omega t} + \epsilon_0 \chi_\omega^{(3)} |\tilde{E}|^2 \tilde{E} e^{i\omega t} + \epsilon_0 \chi_{3\omega}^{(3)} \tilde{E} e^{3i\omega t} + \dots + c.c \right). \quad (7)$$

Where  $\chi_\omega^{(1)}$ ,  $\chi_0^{(2)}$ ,  $\chi_{2\omega}^{(2)}$ ,  $\chi_\omega^{(2)}$  and  $\chi_{3\omega}^{(3)}$  are the linear, second harmonic generation, optical rectification, third order and third harmonic generation susceptibilities, respectively. Due to the inversion symmetry of the system under study, the even orders of susceptibility are zero and  $\chi^{(2)}$  vanishes identically [44]. Therefore, the analytical expressions for the linear and nonlinear optical susceptibilities for a two-level system are given by [45, 46]

$$\epsilon_0 \chi^{(1)}(\omega) = \frac{\sigma_v |M_{12}|^2}{E_{21} - \hbar\omega - i\hbar\Gamma_{12}}, \quad (8)$$

and

$$\epsilon_0 \chi^{(3)}(\omega) = \frac{\sigma_v |M_{12}|^2 |E|^2}{E_{21} - \hbar\omega - i\hbar\Gamma_{12}} \left\{ \frac{4|M_{12}|^2}{(E_{21} - \hbar\omega)^2 + (\hbar\Gamma_{12})^2} - \frac{|M_{22} - M_{11}|^2}{(E_{21} - i\hbar\Gamma_{12})(E_{21} - \hbar\omega - i\hbar\Gamma_{12})} \right\}. \quad (9)$$

Where in the above equations,  $\sigma_v$  is the carrier density,  $M_{ij} = \langle i|x, z|j \rangle$  ( $i, j = 1, 2$ ) are the dipole moment matrix elements and  $E_{21} = E_2 - E_1$  is the energy difference between the ground state and the first excited state. Here,  $\Gamma_{12} = 1/\tau$  is the inverse of the relaxation time  $\tau$  [47–49].

In this model studied, the polarization of the incident photon is determined by the transition matrix element. Indeed, the choice of the transition induces a change of the values of the components of the transition matrix element between zero and non-zero values, the transition where only the axial component of  $M_{ij}$  is non-zero induces a polarization along the axis of the nanowire and the transition where only the planar components of  $M_{ij}$  are non-zero induces a polarization perpendicular to its axis.

The electromagnetic field intensity  $I$  is defined as  $I = (2n_r/\mu c)|E|^2$ , where  $n_r$  is the refractive index,  $c$  is the free-space speed of light, and  $\mu$  is the permeability. The AC and the RI changes are related to the susceptibility,  $\chi(\omega)$ , as follows [50, 51]

$$\alpha(\omega) = \omega \sqrt{\frac{\mu}{\epsilon_0 \epsilon_r}} \text{Im}(\epsilon_0 \chi(\omega)), \quad (10)$$

and

$$\frac{\Delta n(\omega)}{n_r} = \text{Re}\left(\frac{\chi(\omega)}{2n_r^2}\right). \quad (11)$$

Then, from Eq. (10), the analytical forms of the linear and the third-order nonlinear ACs are given by [46, 52]

$$\alpha^{(1)}(\omega) = \omega \sqrt{\frac{\mu}{\epsilon_r}} \frac{|M_{12}|^2 \sigma_v \hbar \Gamma_{12}}{(E_{21} - \hbar\omega)^2 + (\hbar\Gamma_{12})^2}, \quad (12)$$

and

$$\alpha^{(3)}(\omega) = -\omega \sqrt{\frac{\mu}{\epsilon_r}} \left( \frac{I}{2\epsilon_0 n_r c} \right) \frac{|M_{12}|^2 \sigma_v \hbar \Gamma_{12}}{[(E_{21} - \hbar\omega)^2 + (\hbar\Gamma_{12})^2]^2} \times \left( 4|M_{12}|^2 - \frac{|M_{22} - M_{11}|^2 [3E_{21}^2 - 4E_{21}\hbar\omega + (\hbar^2\omega^2 - \hbar^2\Gamma_{12}^2)]}{E_{21}^2 + \hbar^2\Gamma_{12}^2} \right). \quad (13)$$

The total AC can be written as

$$\alpha(\omega) = \alpha^{(1)}(\omega) + \alpha^{(3)}(\omega). \quad (14)$$

Similarly, the linear and the third-order nonlinear RI changes are obtained from Eq. (11) by

$$\frac{\Delta n^{(1)}(\omega)}{n_r} = \frac{1}{2n_r^2 \epsilon_0} \frac{|M_{12}|^2 \sigma_v (E_{21} - \hbar\omega)}{(E_{21} - \hbar\omega)^2 + (\hbar\Gamma_{12})^2}, \quad (15)$$

and

$$\frac{\Delta n^{(3)}(\omega)}{n_r} = -\frac{\mu c I}{4n_r^3 \epsilon_0} \frac{|M_{12}|^2 \sigma_v}{[(E_{21} - \hbar\omega)^2 + (\hbar\Gamma_{12})^2]^2} \left( 4(E_{21} - \hbar\omega) |M_{12}|^2 - \frac{|M_{22} - M_{11}|^2}{E_{21}^2} + \hbar^2 \Gamma_{12}^2 [(E_{21} - \hbar\omega)(E_{21}(E_{21} - \hbar\omega) - (\hbar\Gamma_{12})^2 - (\hbar\Gamma_{12})^2 (2E_{21} - \hbar\omega))] \right). \quad (16)$$

The total RI changes can be written as

$$\frac{\Delta n(\omega)}{n_r} = \frac{\Delta n^{(1)}(\omega)}{n_r} + \frac{\Delta n^{(3)}(\omega)}{n_r}. \quad (17)$$

### 3. Numerical results and discussion

In this section, numerical results of the linear and nonlinear optical AC as well as RI changes in  $\text{CuIn}_{1-x}\text{Ga}_x\text{Se}_2$  nanowire for the two levels of an electron in ground and first excited states are given and discussed. As mentioned before, the objective is to reveal the effect of relaxation time, nanowire radius, incident light intensity and Gallium  $x$  mole fraction on the AC and RI in the two aforementioned incident light polarization cases. For this purpose, the following two transitions are considered:  $(n, l, m) = (1, 1, 0)$  to  $(n, l, m) = (1, 1, 1)$  (T-P $\perp$ ) for the polarization perpendicular to the axis of the nanowire, and the transition  $(n, l, m) = (1, 1, 0)$  to  $(n, l, m) = (2, 1, 0)$  (T-P $\parallel$ ) for the polarization parallel to its axis. In order to obtain the effect of each parameter, only one parameter is changed at a time and all other variables are fixed.

#### 3.1. Absorption coefficient (A.C)

We first set all system parameters as follows the incident light intensity is  $I = 3 \times 10^9 \text{ W/m}^2$  for (T-P $\perp$ ), and  $I = 1 \times 10^7 \text{ W/m}^2$  for (T-P $\parallel$ ), the mole fraction of Gallium  $x$  equals 0.3, electron density of the proposed nanowire is  $\sigma_v = 8.15 \times 10^{23} \text{ m}^{-3}$ , the relaxation time  $\tau$  takes the value 0.2 ps, the  $\epsilon_r$  for the system under study is 13.6 and for a CIGS nanowire radius of 10 nm and 400 nm height, Fig. 1.

It can be seen in Fig. 1 that the optical absorption coefficients show a resonance peak at the specific wavelength/energy of the incident photon. This resonance energy corresponds to the energy interval between the energies of the first state and the excited state. The linear AC is positive and independent of the intensity of incident light, whereas third-order nonlinear AC is negative and proportional to the incident light intensity. the total optical AC is significantly reduced by the nonlinear contribution. Moreover, it can be seen that the transition energy is much lower and the value of the total AC is very high in the case of the (T-P $\parallel$ ) transition. Indeed, the creation of the dipole induced by the external excitation in the axial direction is much more favored thanks to the sufficiently large space compared to the narrow space and the increased confinement of the electron in the radial direction. This induces an increase of the absorbed light to reach an order of magnitude of  $10^7 \text{ m}^{-1}$ , contrary to  $10^5 \text{ m}^{-1}$  in the case of the (T-P $\perp$ ).

In order to clearly see the effect of the incident light energy  $I$  on the optical AC of our system, all the parameters are defined as previously indicated and we vary the incident light intensity on which depends the non-linear AC, Fig. 2.

From this figure, we can obtain that the total AC decreases with increasing incident optical intensity  $I$  for both

transitions, and the absorption is strongly bleached at sufficiently high incident optical intensities. When  $I = 0 \text{ W/m}^2$ , the total AC is equal to the linear absorption coefficient. The total optical AC is significantly decreased by the contribution of third-order nonlinear optical AC when  $I \neq 0$ . Therefore, the effect of nonlinearity must be taken into account and becomes increasingly apparent if the incident optical intensity  $I$  is strong enough that the total optical AC can be reduced. When  $I$  exceeds a critical value, the nonlinear term causes a collapse in the center of the total absorption peaks, splitting them into two peaks in the case of (T-P $\perp$ ) and creating a first sharp negative peak and then an enlarged positive peak for (T-P $\parallel$ ), indicating saturation for both cases. This is known as the bleaching effect [51]. When the incident intensity is high enough, the electrons are excited, but they do not have enough time to decay back to their first state. Therefore, the absorption spectrum is saturated.

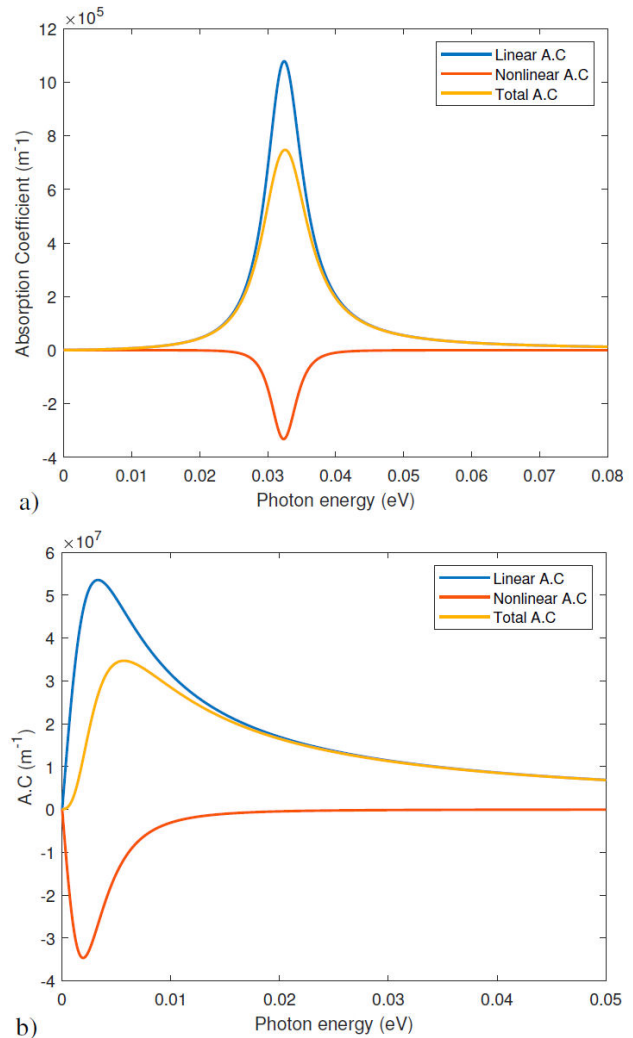


FIGURE 1. Linear, Non linear and total ACs of  $\text{CuIn}_{1-x}\text{Ga}_x\text{Se}_2$  nanowire as function of incident light energy, a) for (T-P $\perp$ ) and b) for (T-P $\parallel$ ).

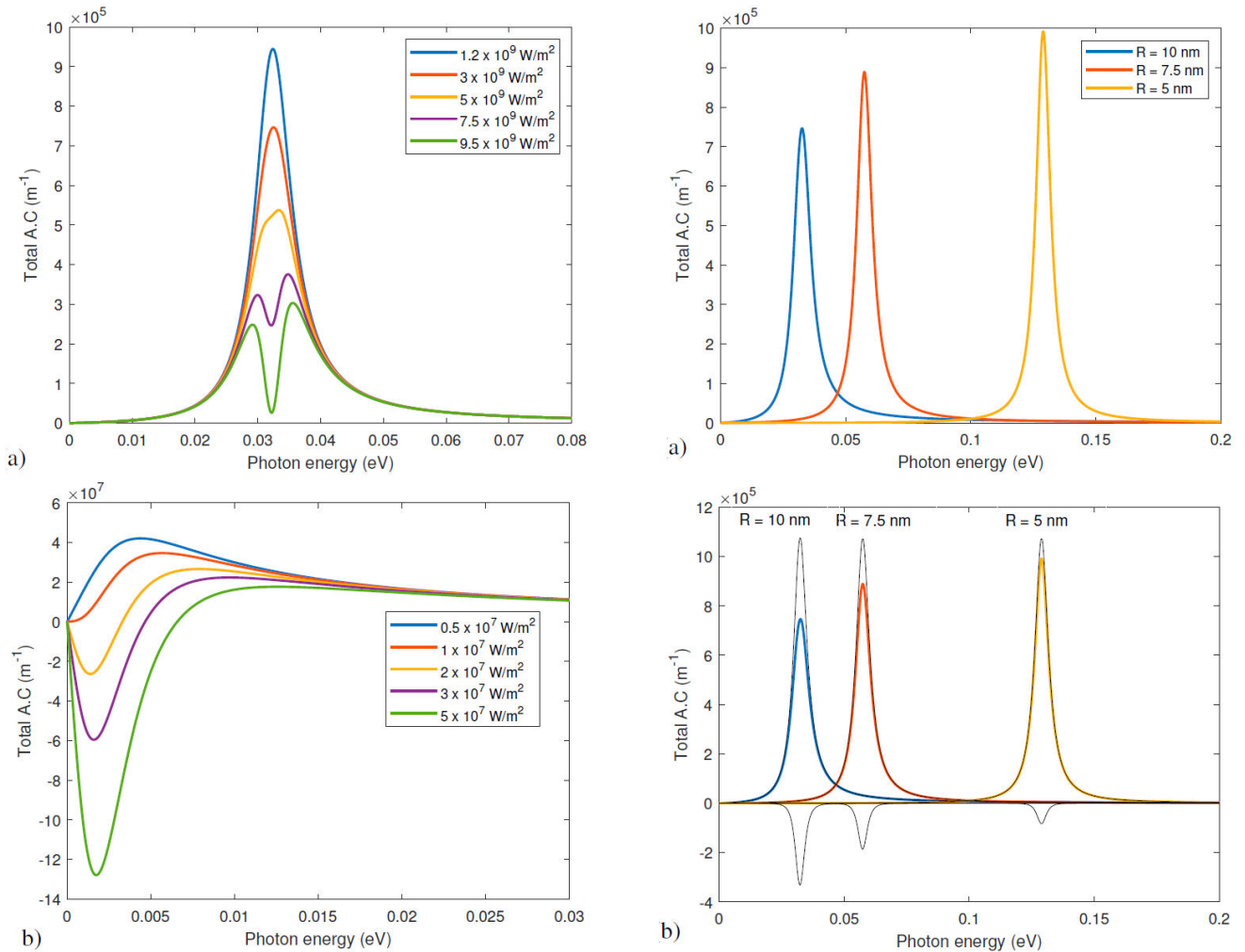


FIGURE 2. Total ACs of  $\text{CuIn}_{1-x}\text{Ga}_x\text{Se}_2$  nanowire as function of energy for multiple values of incident light intensities, a) for (T-P<sub>⊥</sub>) and b) for (T-P<sub>∥</sub>).

The total optical AC of  $\text{CuIn}_{1-x}\text{Ga}_x\text{Se}_2$  nanowire versus incident light energy is shown in Fig. 3, for different values of the wire radius. With the decrease of the wire radius from 10 nm to 5 nm, the resonance energy of the AC is increased, and a blueshift is obtained for (T-P<sub>⊥</sub>), Fig. 3a). This result is due to the electron confinement in space. Indeed, the more the electron is confined in a narrow quantum well the more the energy difference between ground and first excited states increases.

From Fig. 3b), it can also be noticed that the magnitude of the total AC increases with decreasing radius, so that the nonlinear contribution becomes less influential as the wire size becomes smaller and thus the total AC tends toward the linear contribution. This behavior is related to the variations of the energy levels and the elements of the dipole transition matrix as a function of the wire radius. Indeed, according to equation Eq. (12) and Eq. (13), the non-linear optical AC is proportional to the square of the matrix element of the dipole transition, and inversely proportional to the energy difference between the two levels. On the one hand, by decreasing the

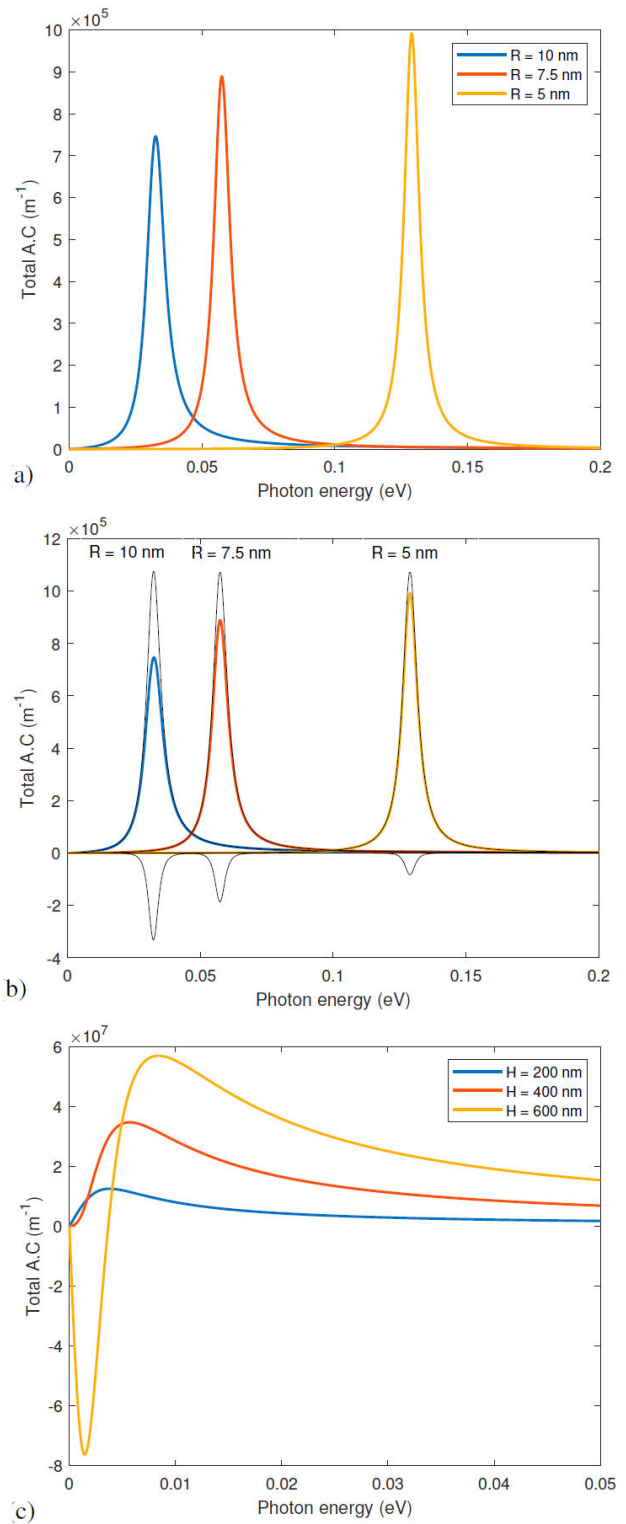


FIGURE 3. a) Total AC versus incident light energy for  $\text{CuIn}_{1-x}\text{Ga}_x\text{Se}_2$  nanowire as function of quantum wire radius for (T-P<sub>⊥</sub>), b) including linear and non linear parts for (T-P<sub>⊥</sub>), and c) for (T-P<sub>∥</sub>).

radius, the creation of the dipole in the radial direction is limited by the size, therefore, the absolute value of the matrix element of the transition decreases. On the other hand, the

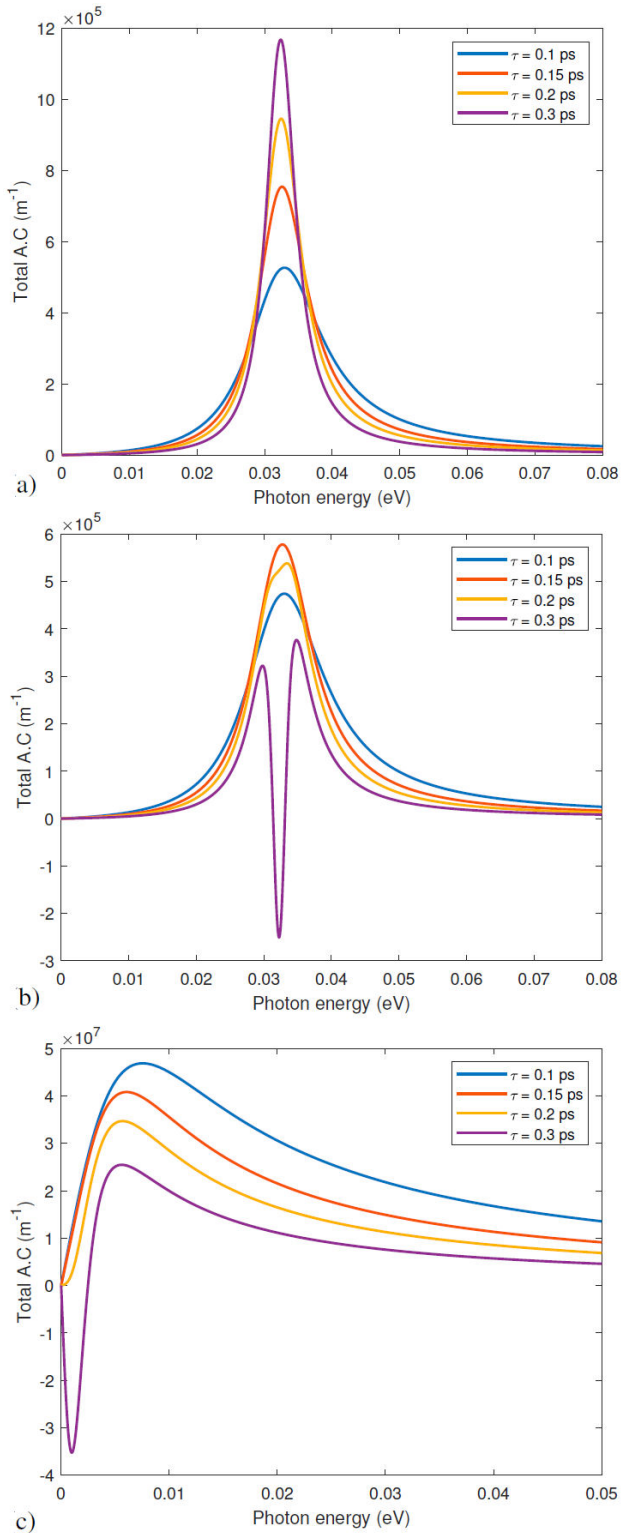


FIGURE 4. a) Total AC versus incident light energy for  $\text{CuIn}_{1-x}\text{Ga}_x\text{Se}_2$  nanowire as function of relaxation time,  $I = 3 \times 10^9 \text{ W/m}^2$  for (T-P $\perp$ ), b)  $I = 5 \times 10^9 \text{ W/m}^2$  for (T-P $\perp$ ), and c) for  $I = 1 \times 10^7 \text{ W/m}^2$  for (T-P $\perp$ ) for (T-P $\parallel$ ).

nonlinear contribution, being inversely proportional to the square of the increasing energy difference between the initial and final states as the radius decreases. Therefore, the non-

linear contribution decreases and the value of the total AC is no longer reduced, it increases and tends towards the linear contribution for small radius values.

Figure 3c) shows the variation of the total AC as a function of the incident photon energy for three values of the nanowire height in the case of the transition (T-P $\parallel$ ). Since the creation of the dipole is favored in the axial direction, we obtain a slight blueshift and the amplitude of the absorption increases significantly as the nanowire height increases. The appearance of a negative peak in the case of large values of the height is due to the fact that the nonlinear contribution of the AC being proportional to the matrix element to the third order. The latter being proportional to the height of the nanowire enhances the effects of nonlinearity.

To highlight the influence of the relaxation time on the total AC, the previous parameters are kept constant except for the relaxation time  $\tau$  which takes the values 0.1 ps, 0.15 ps, 0.2 ps and 0.3 ps, Fig. 4.

In the case of (T-P $\perp$ ) the figure shows the presence of two different behaviors. For relatively low values of the incident light intensity, Fig. 4a), we can see that a continuous increase of the relaxation time leads to a continuous increase of the total AC. On the other hand, when the incident light intensity takes higher values, the effect of the relaxation time becomes different. In fact, the total AC amplitude increases for  $\tau = 0.1$  ps until it reaches a maximum value at in the interval [0.15 ps, 0.2 ps] before collapsing and decreasing, suggesting the presence of an optimal relaxation time in this interval for the specific value of incident light intensity  $I = 5 \times 10^9 \text{ W/m}^2$ , Fig. 4b)). Furthermore, by increasing the relaxation time, the total AC collapses and bleaches rapidly. This result shows that the bleaching effect is more significant when the relaxation time and incident light intensity take higher values. Indeed, unlike the linear part independent of  $I$ , since the nonlinear contribution is proportional to the incident light intensity and inversely proportional to the inverse of the square of the relaxation time, the total AC tends towards the nonlinear part. Besides, the division of the curve into two peaks suggests the creation of an intermediate state between the initial and final state. The transition gives two subtransitions each with a separate resonance peak with a specific transition energy.

In the case of (T-P $\parallel$ ) a similar result of the increase of the nonlinearity is obtained by increasing the relaxation time and the previous interpretations remain valid. However, the amplitude decreases continuously, Fig. 4c).

In order to see how the Ga concentration  $x$  affects the optical properties of this geometry, in In Fig. 5, the total ACs are plotted as a function of the incident photon energy for different values of  $x$  ranging from 0.1 to 0.9, and the other parameters are set previously.

The amplitude of the resonance peak increases with the increase of  $x$  for both transitions and a red shift is also obtained for (T-P $\perp$ ), Fig. 5a). Indeed, in the effective mass approximation, when the gallium concentration  $x$  increases the separate energy levels get closer to each other. The range

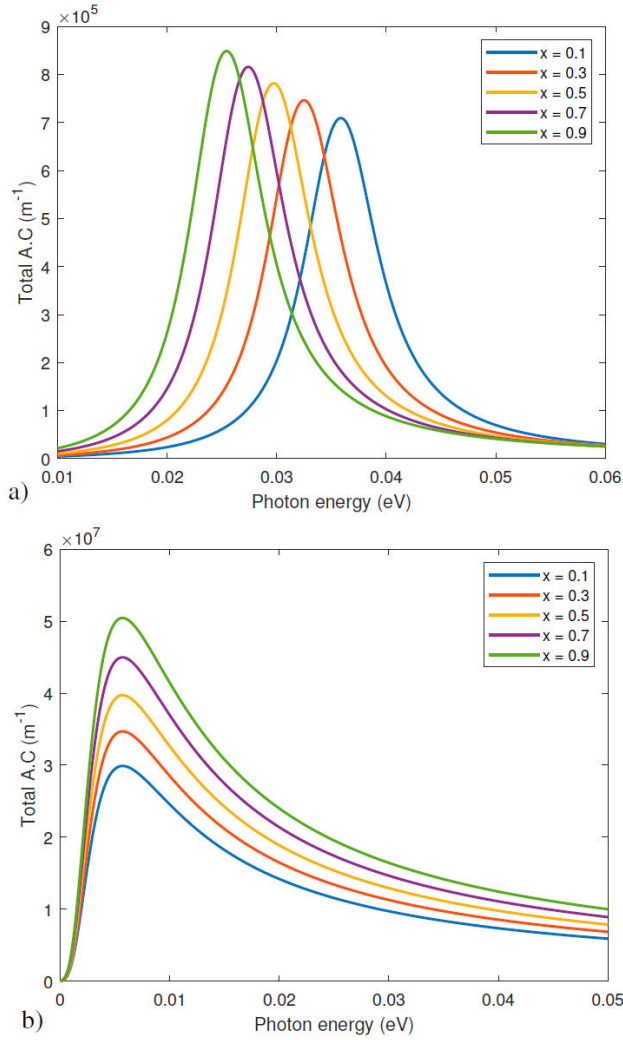


FIGURE 5. Total AC versus incident light energy for  $\text{CuIn}_{1-x}\text{Ga}_x\text{Se}_2$  nanowire as function of Gallium mole fraction  $x$ , a) for (T-P $\perp$ ) and b) for (T-P $\parallel$ ).

of the transition energy  $E_{fi} = E_f - E_i$  becomes narrower and, consequently, the resonance peak of the total AC shifts to lower energies. For the transition (T-P $\parallel$ ), Fig. 5b), the height of the nanowire being very large compared to its radius, the electron is free in the axial direction and the effect of the change of the effective mass due to the increase of  $x$  has a negligible effect on the electron energy. Consequently, the transition energy is unchanged. Moreover, by changing the Ga doping concentration, the charge carrier concentration varies, even by a limited rate, but this variation has an impact on the total AC leading to an increase of its amplitude when the Ga concentration increases.

### 3.2. Refractive Index changes (R.I)

As in the previous section, we first define all the variables as follows: the incident light intensity is  $I = 3 \times 10^9 \text{ W/m}^2$  for (T-P $\perp$ ), and  $I = 1 \times 10^7 \text{ W/m}^2$  for (T-P $\parallel$ ). The Gallium mole fraction is  $x = 0.3$ , the relaxation time  $\tau$  is taken equal to 0.2 ps, the electron density of the proposed nanowire is

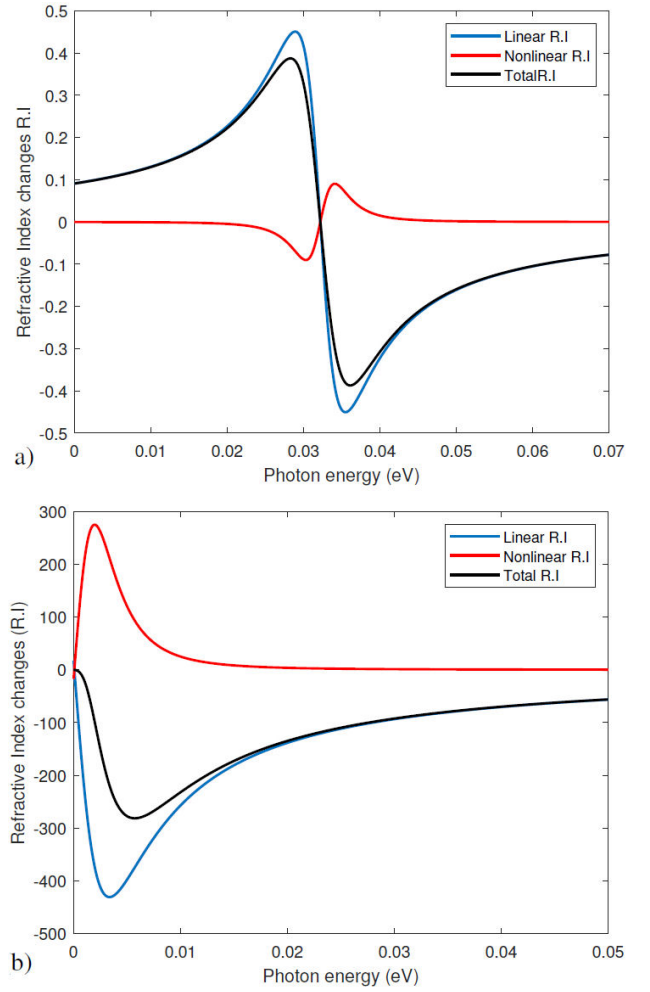


FIGURE 6. Linear, non linear and total RI changes of  $\text{CuIn}_{1-x}\text{Ga}_x\text{Se}_2$  nanowire as function of incident light energy, a) for (T-P $\perp$ ) and b) for (T-P $\parallel$ ).

$\sigma_v = 8.15 \times 10^{23} \text{ m}^{-3}$ , the relative permittivity  $\epsilon_r$  takes the value 13.6 and for a CIGS wire radius of 10 nm and 400 nm height. The linear, nonlinear, and total RI changes versus incident light energy is shown in Fig. 6.

The linear part of the RI changes is dominant over the nonlinear part, so the effect of the nonlinear contribution on the total RI changes is less apparent, for the transition (T-P $\perp$ ) and the rate of change relative to  $n_r$  is low. In contrast to the transition (T-P $\parallel$ ) where the total RI changes tend to the nonlinear RI and the rate of change with respect to  $n_r$  is very high. Moreover, at the resonance photon energy, the linear, third-order nonlinear, and total RI changes are equal to zero. Further on, the transition energy in the (T-P $\parallel$ ) case being close to zero the RI change curve keeps only the right hand side and the left hand side vanishes. It is noteworthy that most of the interpretations given in the case of the AC remain valid for the case of the RI changes.

Figure 7 illustrates the effect of structure size on the variation of the RI as a function of incident photon energy. Similar to the case of total AC seen earlier, as the wire radius decreases, we also get a shift of the peaks to higher energies

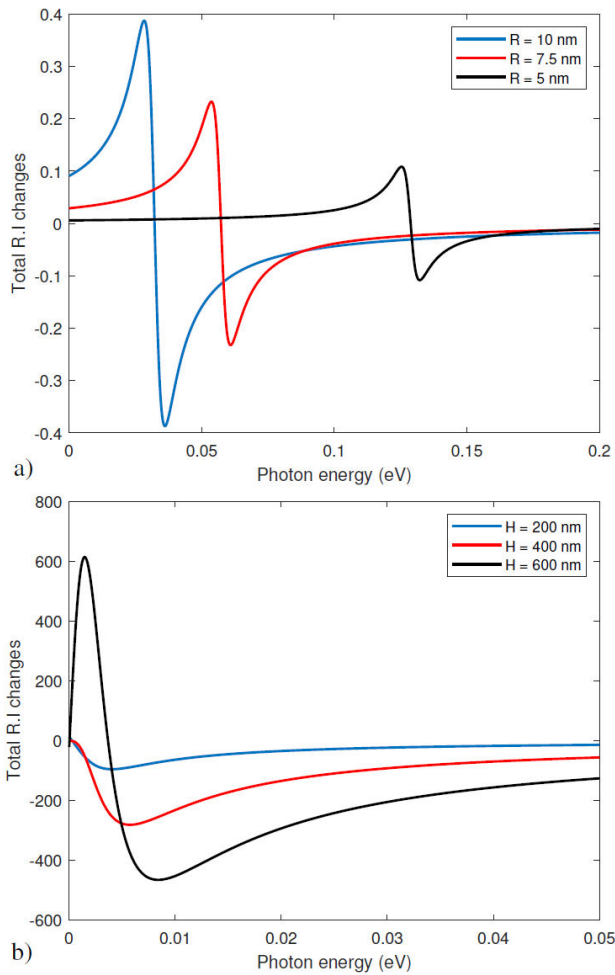


FIGURE 7. Variation of the total refractive index changes of  $\text{CuIn}_{1-x}\text{Ga}_x\text{Se}_2$  nanowire as function of different values of wire radius for a) (T-P $_{\perp}$ ), and b) for (T-P $_{\parallel}$ ).

(blueshift), Fig. 7a), due to the increase in the energy difference between the ground state and the first excited state. This result is in agreement with the results of previous studies in the literature showing that the energy of electrons increases when they are strongly confined. However, the amplitude of the resonance peaks of the total RI change decreases. This shows that the smaller the size of the structure, the more the excitation barely changes the refractive index of the material, and thus the refractive index is strongly dependent on the geometry of the system. Concerning the second transition, a very low energy shift is obtained, and the more the height of the nanowire increases, the more the rate of change increases drastically and the effect of the non-linear contribution is more pronounced, Fig. 7b).

In order to see how the relaxation time affects the optical properties of our system, the variation of the total RI change as a function of the incident photon energy is shown in Fig. 8, for different values of relaxation time. The other parameters are fixed as described above.

In contrast to the total AC where an optimal value of the relaxation time is observed for a specific value of the incident

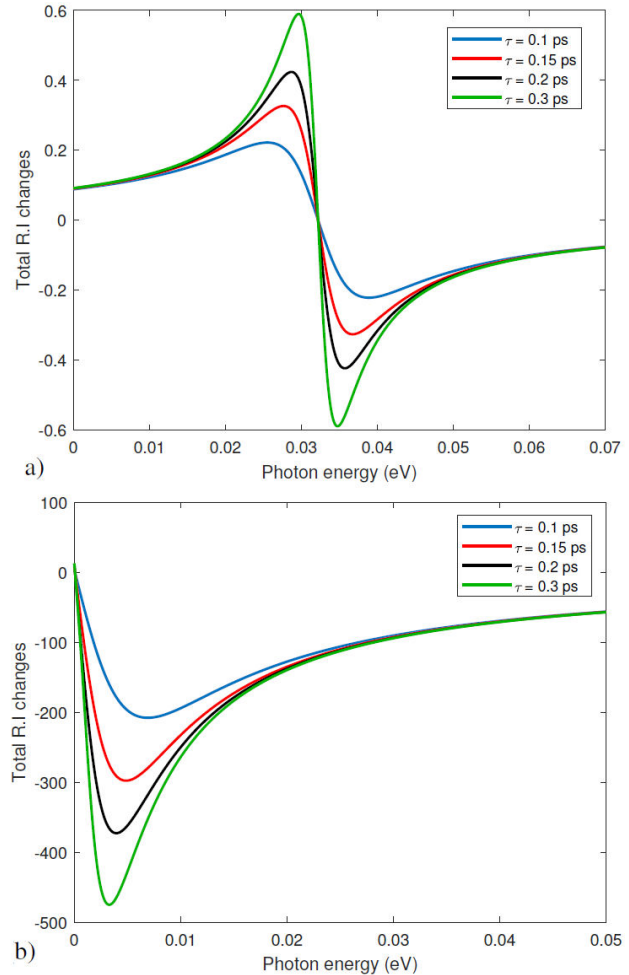


FIGURE 8. Variation of the total RI changes of  $\text{CuIn}_{1-x}\text{Ga}_x\text{Se}_2$  nanowire as function of different values of relaxation time for a) (T-P $_{\perp}$ ), and b) for (T-P $_{\parallel}$ ).

photon intensity, here a continuous increment of the relaxation time leads to a continuous increment of the amplitude of the changes in the total RI. Moreover, by increasing the relaxation time, the resonance peak becomes sharper without causing splitting of the curve as in the case of total AC, and the change in total IR is extremely close to the linear contribution. This applies to both transitions, Fig. 8.

The dependence of RI changes on Ga concentration  $x$  is demonstrated by plotting the total RI change as a function of incident photon energy for multiple values of  $x$  ranging from 0.1 to 0.9, and other parameters held constant, Fig. 9.

The results show that by increasing the Ga concentration  $x$ , the total RI resonance peaks are subjected to a redshift for (T-P $_{\perp}$ ). This is due to the fact that the energy interval between the ground state and the first excited state decreases as the Ga concentration increases, as discussed in the previous section. Similarly, the magnitude of the change in total RI increases with decreasing  $x$  concentration of Ga, and tends toward the linear RI change. No energy shift is obtained for (T-P $_{\parallel}$ ). The reasons given for the total AC remain valid for both cases.

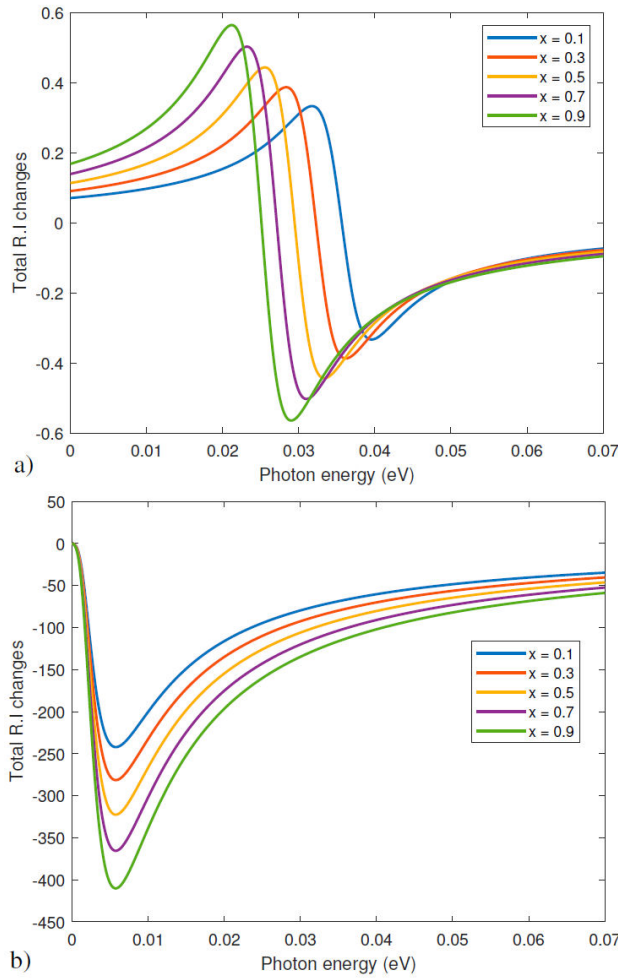


FIGURE 9. Total RI changes of  $\text{CuIn}_{1-x}\text{Ga}_x\text{Se}_2$  nanowire versus incident light energy as function of Gallium mole fraction  $x$  for a) (T-P $_{\perp}$ ), and b) for (T-P $_{\parallel}$ ).

To highlight the effect of incident photon intensity on RI changes for the studied structure, the total RI changes are plotted versus incident photon energy for different intensity values, Fig. 10. Other parameters are defined as previously shown.

The figure shows the reduction in the amplitude of the total RI resonance peaks as the incident optical intensity increases for (T-P $_{\perp}$ ). This is due to the contribution of the third-order nonlinear variation of the RI, which is strongly related to the incident optical intensity, as shown in Eq. (16), in contrast to the linear variation of the RI, which is independent of the incident optical intensity. This contribution of the nonlinear part is most evident when a critical intensity is reached, where a split is created in the curve, indicating the dominance of the nonlinear part on the total RI changes. A similar behavior is obtained for the transition (T-P $_{\parallel}$ ), but in a more accrued manner.

In both the AC and RI changes cases the results obtained are in good agreement with the results published in the literature for different semiconductor nanostructures [53–57].

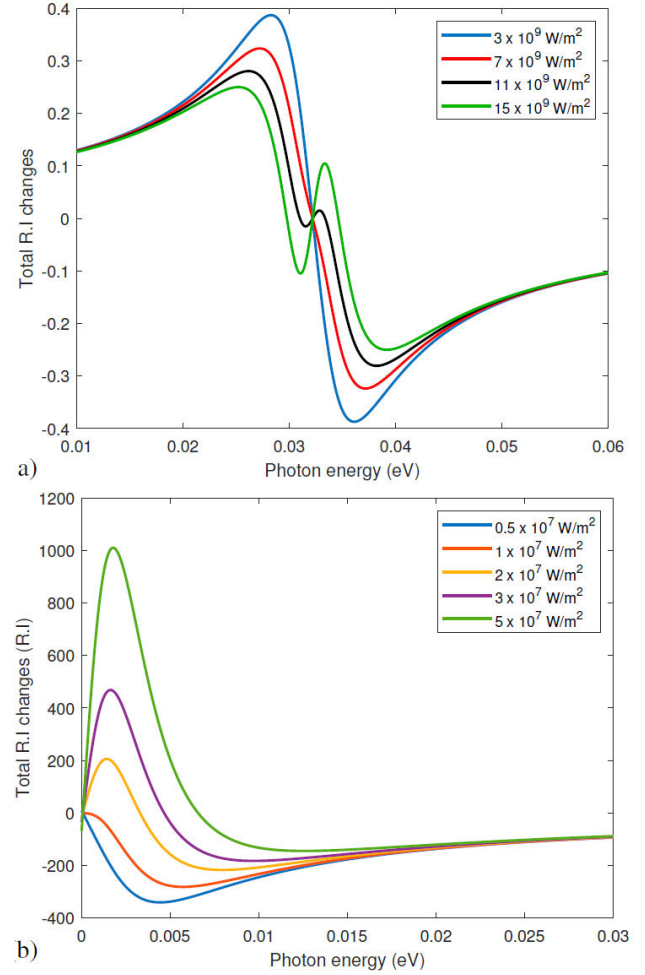


FIGURE 10. Total RI changes of  $\text{CuIn}_{1-x}\text{Ga}_x\text{Se}_2$  nanowire as function of different values of incident light intensities for a) (T-P $_{\perp}$ ), and b) for (T-P $_{\parallel}$ ).

## 4. Conclusion

In this paper, the effects of incident light intensity, relaxation time, nanowire radius, and Ga mole fraction  $x$  on the linear, nonlinear, and total optical AC and RI change in the free  $\text{CuIn}_{1-x}\text{Ga}_x\text{Se}_2$  nanowire are theoretically investigated for the intersubband transition from the ground state to the first excited state. The two transitions considered in this work represent the two cases of polarization of the incident light: perpendicular and parallel to the nanowire axis. The results obtained show that the nonlinear contribution to the total AC is mainly influenced by the incident light intensity first, and then by the change in relaxation time. The amplitude of the peaks in total AC and total RI decreases rapidly with increasing incident light intensity until reaching a saturation point where the nonlinear aspect becomes stronger than the linear aspect. The increase of the relaxation time leads to a decrease of the amplitude of the peaks in total AC and an opposite behaviour for total RI. In addition, the positions of the peaks and their transition energies are mainly influenced by

the mole fraction  $x$  of Ga and nanowire size for the perpendicular polarization case. While in the case of axial polarization no effect is obtained on the transition energy, however, the changes in the amplitude are more increased and pronounced. Thus, it can be stated that the relaxation time and the incident light intensity are the parameters favoring the appearance of nonlinear phenomena while the nanowire size and the Ga concentration influence the transition energy. Consequently, the polarization of the incident light perpendicular to the axis of the wire allows to obtain linear and non-

linear optical properties tunable by the size of the structure and the doping rate but gives a low absorption coefficient due to the confinement of the charge carriers in the radial direction. On the other hand, the polarization along the nanowire axis allows to obtain very high absorption rates at very low transition energies thanks to the non confinement of charge carriers in the axial direction favoring the creation of dipoles but the control of the optical properties through the parameters of the system is reduced.

1. B. K. Hughes, J. M. Luther and M. C. Beard, *ACS Nano*, **6** (2012) 4573, <https://doi.org/10.1021/nn302286w>.
2. Yong K. *et al.*, *Nano Lett.* **6** (2006) 599, <https://doi.org/10.1021/nl052189o>.
3. D. Abouelaoualim, *Acta Phys. Pol. A*, **112** (2007) 49, <https://doi.org/10.12693/APHYSPOLA.112.49>.
4. A. Davydov, *Semiconductor Nanowires: Opportunities and Challenges*, NIST workshop on WWW, [https://www.nist.gov/system/files/documents/mml/msed/thermodynamics\\_kinetics/Davydov-Semiconductor-Nanowires.pdf](https://www.nist.gov/system/files/documents/mml/msed/thermodynamics_kinetics/Davydov-Semiconductor-Nanowires.pdf)
5. A. I. Hochbaum and P. Yang, *Semiconductor Nanowires for Energy Conversion*, *Nano Lett. Pol. A*, **10** (2010) 529-1536, <https://doi.org/10.1021/cr900075v>.
6. M. S. Tame *et al.*, *Nat. Phys.* **9** (2013) 329, <https://doi.org/10.1038/nphys2615>.
7. C. Sikorski and U. Merkt, *Phys. Rev. Lett.* **62** (1989) 2164, <https://doi.org/10.1103/PhysRevLett.62.2164>.
8. R. C. Ashoori *et al.*, *Phys. Rev. Lett.* **71** (1993) 613, <https://doi.org/10.1103/PhysRevLett.71.613>.
9. W. Y. Ruan, Y. Y. Liu, C. G. Bao, and Z. Q. Zhang, *Phys. Rev. B* **51** (1995) 7942, <https://doi.org/10.1103/PhysRevB.51.7942>.
10. U. De Giovannini, F. Cavaliere, R. Cenni, M. Sassetti, and B. Kramer, *Phys. Rev. B* **77** (2008) 035325, <https://doi.org/10.1103/PhysRevB.77.035325>.
11. Y. Cui, Z. Zhong, D. Wang, W. U. Wang, and C. M. Lieber, *High performance silicon nanowire field effect transistors*, *Nan. Lett.* **3** (2003) 149, <https://doi.org/10.1021/nl0258751>.
12. Y. Huang, X. Duan, and C. M. Lieber, *Nanowires for integrated multicolor nanophotonics*, *Small* **1**, (2005) 142-147, <https://doi.org/10.1002/smll.200400030>.
13. Y. Cui, Q. Wei, H. Park, and C. M. Lieber, *Nanowires nanosensors for highly sensitive and selective detection of biological and chemical species*, *Science*, **293** (2001) 1289, <https://doi.org/10.1126/science.1062711>.
14. G. Zheng, W. Lu, S. Jin, and C. M. Lieber, *Synthesis and fabrication of highperformance n-type silicon nanowire transistors*, *Adv. Mater.*, **16** (2004) 1890, <https://doi.org/10.1002/adma.200400472>.
15. F. Qian *et al.*, *Gallium nitride-based nanowire radial heterostructures for nanophotonics*, *Nano. Lett.*, **4** (2004) 1975, <https://doi.org/10.1021/nl0487774>.
16. C. Y. Nam *et al.*, *Diameter-dependent electromechanical properties of GaN nanowires*, *Nano. Lett.*, **6** (2006) 153, <https://doi.org/10.1021/nl051860m>.
17. Y. Zhang, A. Kolmakov, S. Chretien, H. Metiu, and M. Moskovits, *Control of catalytic reactions at the surface of a metal oxide nanowire by manipulating electron density inside it*, *Nan. Lett.*, **4** (2004) 403, <https://doi.org/10.1021/nl034968f>.
18. G. Shen and D. Chen, *One-Dimensional Nanostructures and Devices of II-V Group Semiconductors*, *Nanoscale Res Lett.*, **4** (2009) 779, <https://doi.org/10.1007/s11671-009-9338-2>.
19. J. Wang, M. S. Gudiksen, X. Duan, Y. Cui and C. M. Lieber, *Highly polarized photoluminescence and photodetection from single indium phosphide nanowires*, *Science* **293** (2001) 1455, <https://doi.org/10.1126/science.1062340>.
20. A. Casadei *et al.*, *Polarization response of nanowires a la carte*, *Sci. Rep.* **5** (2015) 7651, <https://doi.org/10.1038/srep07651>.
21. M. Heiss and A. Fontcuberta i Morral, *Fundamental limits in the external quantum efficiency of single nanowire solar cells*, *Applied Physics Letters*, **99** (2011) 263102, <https://doi.org/10.1063/1.3672168>.
22. G. Chen *et al.*, *Optical antenna effect in semiconducting nanowires*, *Nano Letters* **8** (2008) 1341, <https://doi.org/10.1021/nl080007v>.
23. S. Wagner, J. Shay, P. Migliorato and H. Hasper, *Appl. Phys. Lett.*, **25** (1974) 434, <https://doi.org/10.1063/1.1655537>.
24. H.W. Schock and R.Noufi, *Prog. Photovoltaics*, **8** (2000) 151, [https://doi.org/10.1002/\(SICI\)1099-159X\(200001/02\)8:1<151::AID-PIP302>3.0.CO;2-Q](https://doi.org/10.1002/(SICI)1099-159X(200001/02)8:1<151::AID-PIP302>3.0.CO;2-Q).
25. P. Jackson *et al.*, *Prog. Photovoltaics*, **19** (2011) 894, <https://doi.org/10.1002/pip.1078>.
26. Q. Cao *et al.*, *Adv. Energy Mater.* **1** (2011) 845, <https://doi.org/10.1002/aenm.201100344>.

27. A. Chirila *et al.*, *Nat. Mater.*, **10** (2011) 857, <https://doi.org/10.1038/nmat3122>.
28. J. Tang, Z. Huo, S. Brittan, H. Gao and P. Yang, *Nat. Nanotechnol.* **6** (2011) 568, <https://doi.org/10.1038/nnano.2011.139>.
29. A. Segev, A. Saar, J. Oiknine-Schlesinger and E. Ehrenfreund, *Superlattices Microstruct.* **19** (1996) 47, <https://doi.org/10.1006/spmi.1996.0007>.
30. N. Sei, H. Ogawa and K. Yamada, *Opt. Lett.* **34** (2009) 1843, <https://doi.org/10.1364/OL.34.001843>.
31. U. Woggon, *Optical Properties of Semiconductor Quantum Dots* Springer-Verlag, Berlin, (1997), <https://link.springer.com/book/10.1007/BFb0119351>.
32. S. Nizamoglu and H. V. Demir, *Opt. Express* **16** (2008) 3515, <https://doi.org/10.1364/OE.16.003515>.
33. W. Xie, *J. Phys.: Condens. Matter* **20** (2008) 365213, <https://doi.org/10.1088/0953-8984/20/36/365213>.
34. M. Sahin, *Phys. Rev. B* **77** (2008) 045317, <https://doi.org/10.1103/PhysRevB.77.045317>.
35. S. Yilmaz and H. Safak, *Int. J. (Mod. Phys. B)* **23** (2009) 2127, <https://doi.org/10.1142/S0217979209052030>.
36. Y.C. Zhou, G.-P. He and Z.-M. Wang, *Phys. Lett. A* **229** (1997) 379, [https://doi.org/10.1016/S0375-9601\(97\)00169-2](https://doi.org/10.1016/S0375-9601(97)00169-2).
37. R. W. Boyd, *Nonlinear Optics Academic*, San Diego, (2003), <https://www.elsevier.com/books/nonlinear-optics/boyd/978-0-12-121682-5>.
38. P. Kumari, S. Sinha, and L. K. Mishra, *A theoretical evaluation of changes of refractive index as a function of photon energy for different incident optical intensities and fixed length of quantum wire*, *Journal of Pure Applied and Industrial Physics*, **7** (2017) 264, <http://physics-journal.org/download/Priyanka-KumariSangeeta-Sinha-and-L-K-Mishra/PHSV07I06P0275.pdf>.
39. G. Liu, K. Guo, L. Xie, Z. Zhang, and L. Lu, *Tunability of linear and nonlinear optical absorption in laterally-coupled  $\text{Al}_x\text{Ga}_{1-x}\text{As}/\text{GaAs}$  quantum wires*, *Journal of Alloys and Compounds*, **746** (2018) 653, <https://doi.org/10.1016/j.jallcom.2018.02.333>.
40. N. Arunachalam, A. John Peter, and C. K. Yoo, *Exciton optical absorption coefficients and refractive index changes in a strained  $\text{InAs}/\text{GaAs}$  quantum wire: The effect of the magnetic field*, *Journal of Luminescence*, **132** (2012) 1311, <https://doi.org/10.1016/J.JLUMIN.2012.01.003>.
41. M. Karimi and M. Hosseini, *Electric and magnetic field effects on the optical absorption of elliptical quantum wire*, *Superlattices and Microstructures*, **111** (2017) 96, <https://doi.org/10.1016/j.spmi.2017.06.019>.
42. G. Rezaei, M.R.K. Vahdani and B. Vaseghi, *Physica B*, **406**, (2011) 1488, <https://doi.org/10.1016/j.physb.2011.01.053>.
43. M.R.K. Vahdani, *The effect of the electronic intersubband transitions of quantum dots on the linear and nonlinear optical properties of dot-matrix system*, *Superlattices Microstruct.* **76** (2014) 326, <https://doi.org/10.1016/j.spmi.2014.09.023>.
44. Robert W. Boyd, *Nonlinear Optics* (Second Edition), Academic Press, (2003) 2-3.
45. A. El Kadadra, K. Fellaoui, D. Abouelaoualim and A. Oueriagli, *Optical absorption coefficients in  $\text{GaN}/\text{Al}(\text{Ga})\text{N}$  double inverse parabolic quantum wells under static external electric field*, *Mod. Phys. Lett. B* **30** (2016) 1650165, <https://doi.org/10.1142/S0217984916501657>.
46. M.R.K. Vahdani and G. Rezaei, *Phys. Lett. A*, **373** (2009) 3079, <https://doi.org/10.1016/j.physleta.2009.06.042>.
47. B. Cakir, Y. Yakar and A. Ozmen, *J. Lumin.* **132** (2012) 2659, <https://doi.org/10.1016/j.jlumin.2012.03.065>.
48. W. Xie, *Physica B* **405** (2010) 3436, <https://doi.org/10.1016/j.physb.2010.05.019>.
49. K. Fellaoui, A., Oueriagli and D. Abouelaoualim, *Indian J. Phys.* **93** (2019) 1353, <https://doi.org/10.1007/s12648-019-01378-x>.
50. K.J. Kuhn *et al.*, *J. Appl. Phys.*, **70** (1991) 5010, <https://doi.org/10.1063/1.349005>.
51. D. Ahn and S.L. Chuang, *Calculation of linear and nonlinear intersubband optical absorptions in a quantum well model with an applied electric field*, *IEEE J. Quantum Electron.*, **QE-23** (1987) 2196, <https://doi.org/10.1109/JQE.1987.1073280>.
52. G. Rezaei, M.R.K. Vahdani and M. Barati, *Polaron effects on the intersubband optical absorption coefficient and refractive index changes of an infinite confining potential quantum box*, *J. Nanoelectron. Optoelectron.* **3**, (2008) 159. <https://doi.org/10.1166/jno.2008.208>.
53. M. Kouhi, *Nonlinear optical absorption in the core shell nanowire*, *International Journal of Modern Physics B* **31** (2017) 1750164, <https://doi.org/10.1142/S0217979217501648>.
54. A. Zamani, Gh. Safarpour, L. Safaei, E. Niknam and M. Novzari, *The linear and nonlinear optical properties of a bulged  $\text{GaAs}$  nanowire*, *Superlattices and Microstructures* **81** (2015) 129, <https://doi.org/10.1016/j.spmi.2015.01.023>.
55. Gh. Safarpour, M. Novzari, M.A. Izadi and S. Yazdanpanahi, *The linear and nonlinear optical properties of  $\text{GaAs}/\text{GaAlAs}$  nanowire superlattices*, *Superlattices and Microstructures* **75** (2014) 725, <https://doi.org/10.1016/j.spmi.2014.08.020>.
56. M. Solaimani, *Nonlinear optical absorption of a two electron  $\text{GaN}/\text{AlN}$  constant total effective radius multi-shells quantum rings*, *Journal of Nonlinear Optical Physics and Materials* **23** (2014) 1450050, <https://doi.org/10.1142/S0218863514500507>.
57. M. Tshipa, *Optical Properties of  $\text{GaAs}$  Nanowires with an Electric Potential That Varies Inversely with the Square of the Radial Distance*, *Hindawi Advances in Condensed Matter Physics* (2019), Article ID 3478506, <https://doi.org/10.1155/2019/3478506>.